Supplementary Information

Elevated synaptic PKA activity and abnormal striatal dopamine signaling in *Akap11* mutant mice, a genetic model of schizophrenia and bipolar disorder

Bryan J. Song[1,#,*], Yang Ge[1,#], Ally Nicolella[1], Min Jee Kwon[1], Bart Lodder[2,3], Kevin Bonanno[4], Antia Valle-Tojeiro[4], Nolan D. Hartley[1,5], Kira Perzel Mandell[1], John Adeleye[1], Deeksha Misri[1], Chuhan Geng[1], Sahana Natarajan[1], Inès Picard[1], Nate Shepard[1], Alyssa Hall[1], Jiawen Tian[1,5], Sameer Aryal[1], Zohreh Farsi[1], Xiao-Man Liu[1], Nader Morshed[1,5], Naeem M. Nadaf[1], Horia Pribiag[1], Sean K. Simmons[1], D. R. Mani[4], Beth Stevens[1,6,7], Prabhat S. Kunwar[1], Zhanyan Fu[1,5], Evan Z. Macosko[1,8], Joshua Z. Levin[1], Bernardo L. Sabatini[2], Steven A. Carr[4], Borislav Dejanovic[1,9], Hasmik Keshishian[4], Adam J. Granger[1,*] & Morgan Sheng[1,10,*]

1 The Stanley Center for Psychiatric Research, The Broad Institute of MIT and Harvard, Cambridge, MA, USA
2 Department of Neurobiology, Howard Hughes Medical Institute, Harvard Medical School, Boston, MA, USA
3 Brain Center, Department of Translational Neuroscience, University Medical Center Utrecht and University Utrecht, the Netherlands
4 The Proteomics Platform, The Broad Institute of MIT and Harvard, Cambridge, MA, USA
5 Yang Tan Collective and McGovern Institute for Brain Research, Department of Brain and Cognitive Sciences, Massachusetts Institute of Technology, Cambridge, MA, USA
6 F.M. Kirby Neurobiology Center, Boston Children's Hospital, Boston, MA, USA
7 Howard Hughes Medical Institute, Boston Children's Hospital, Boston, MA, USA
8 Massachusetts General Hospital, Department of Psychiatry, Boston, MA, USA
9 Currently: Vigil Neuroscience, Cambridge, MA, USA
10 Department of Brain and Cognitive Sciences, Massachusetts Institute of Technology, Cambridge, MA, USA
# Equal Contributions
*Correspondence: bsong@broadinstitute.org, agranger@broadinstitute.org, msheng@broadinstitute.org

Supplementary Figures and Figure Legends

Supplementary Figure 1

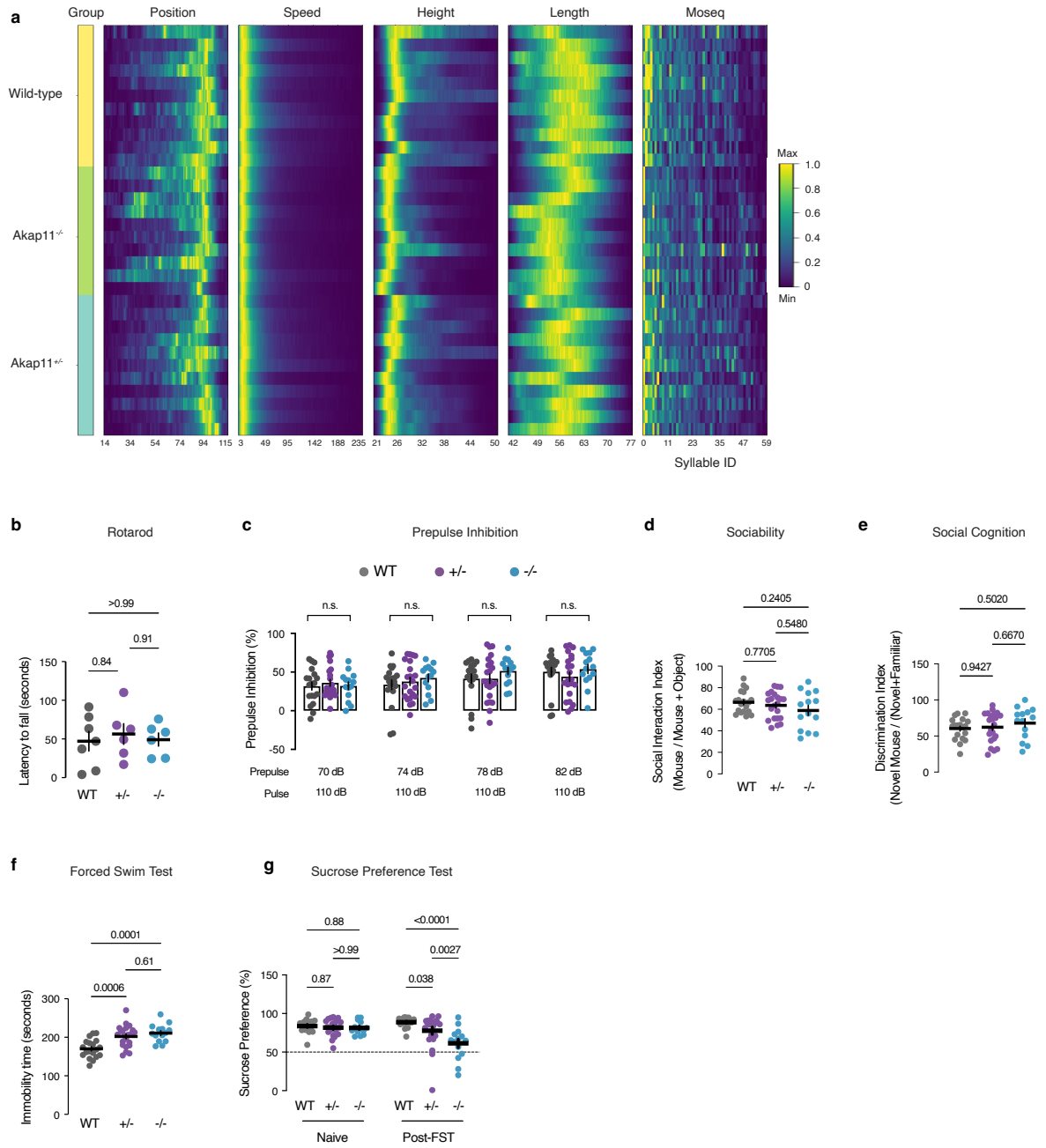

Supplementary Figure 1: Behavioral survey of *Akap11* mutant mice, related to Fig. 1.
a, Heatmaps showing the position, speed, height, length, or MoSeq (syllable usage) by each mouse, grouped into WT (top), *Akap11*$^{+/-}$ (bottom), and *Akap11*$^{-/-}$ (middle).
b, Average latency to fall across 4 rotarod test trials.
c, Prepulse inhibition to an acoustic stimulus, measured as a percentage of accelerometer response to the test pulse, relative to a less intense prepulse.
d, Performances of WT and *Akap11* mutant mice during the three-chamber test for sociability. Social interaction index is defined as: time(mouse)/(time(mouse) + time(object)) x 100%.
e, Performances of WT and *Akap11* mutant mice during the three-chamber test for social cognition. Discrimination index is defined as: time(novel)/time(novel) + time(familiar) x 100%.

f, Immobility duration during the forced swim test (FST).
g, Sucrose preference of *Akap11* mutant and WT animals before and after undergoing FST.
b-g, data are represented as mean +/- SEM
b,d,e,f, One-way ANOVA with Tukey's post hoc test. See Supplementary Data 1 for statistics.
c,g, Repeated measures two-way ANOVA with Tukey's post hoc test. See Supplementary Data 1 for statistics.

Supplementary Figure 2

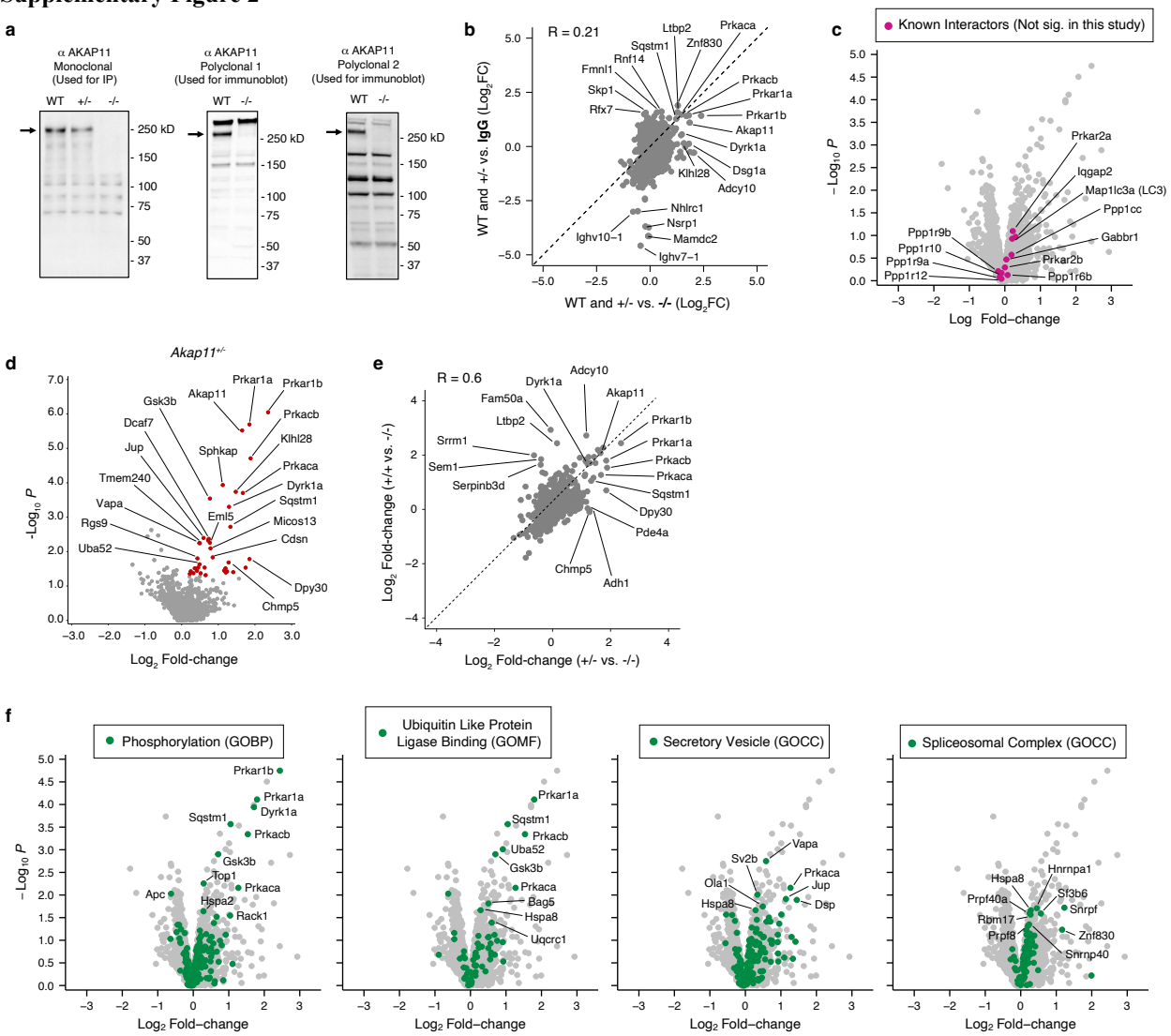

Supplementary Figure 2: AKAP11-interacting proteins and pathways in WT and in *Akap11*$^{+/-}$, related to Fig. 2.
a, Immunoblots of mouse cortex total lysate using AKAP11 antibodies used in this study.
b, Log_2FC scatterplot comparing *Akap11*$^{-/-}$ vs. IgG as controls for AKAP11 IP. In these data, AKAP11 IP in WT and *Akap11*$^{+/-}$ animals were compared together against AKAP11 IP in *Akap11*$^{-/-}$ animals or IgG in WT animals.
c, Volcano plot of AKAP11 CoIP-MS (WT vs. *Akap11*$^{-/-}$). Highlighted in magenta are proteins that have been previously reported to interact with AKAP11, but were not significantly enriched in this study.
d, Volcano plot of AKAP11 coIP-MS, comparing IP in *Akap11*$^{+/-}$ vs. *Akap11*$^{-/-}$ cortex. Proteins with nominal *P* value < 0.05 and $Log_2FC > 0$ are colored red.
e, Log_2FC scatterplots comparing all proteins detected by AKAP11 IP in WT versus *Akap11*$^{+/-}$.
f, Volcano plot of AKAP11 coIP-MS. Highlighted in green are proteins within gene ontology (GO) pathways that were significantly found to be enriched by GSEA. (GOBP, Gene Ontology Biological Process; GOCC, Gene Ontology Cellular Component; GOMF, Gene Ontology Molecular Function).
b,e, R = Pearson correlation.

Supplementary Figure 3

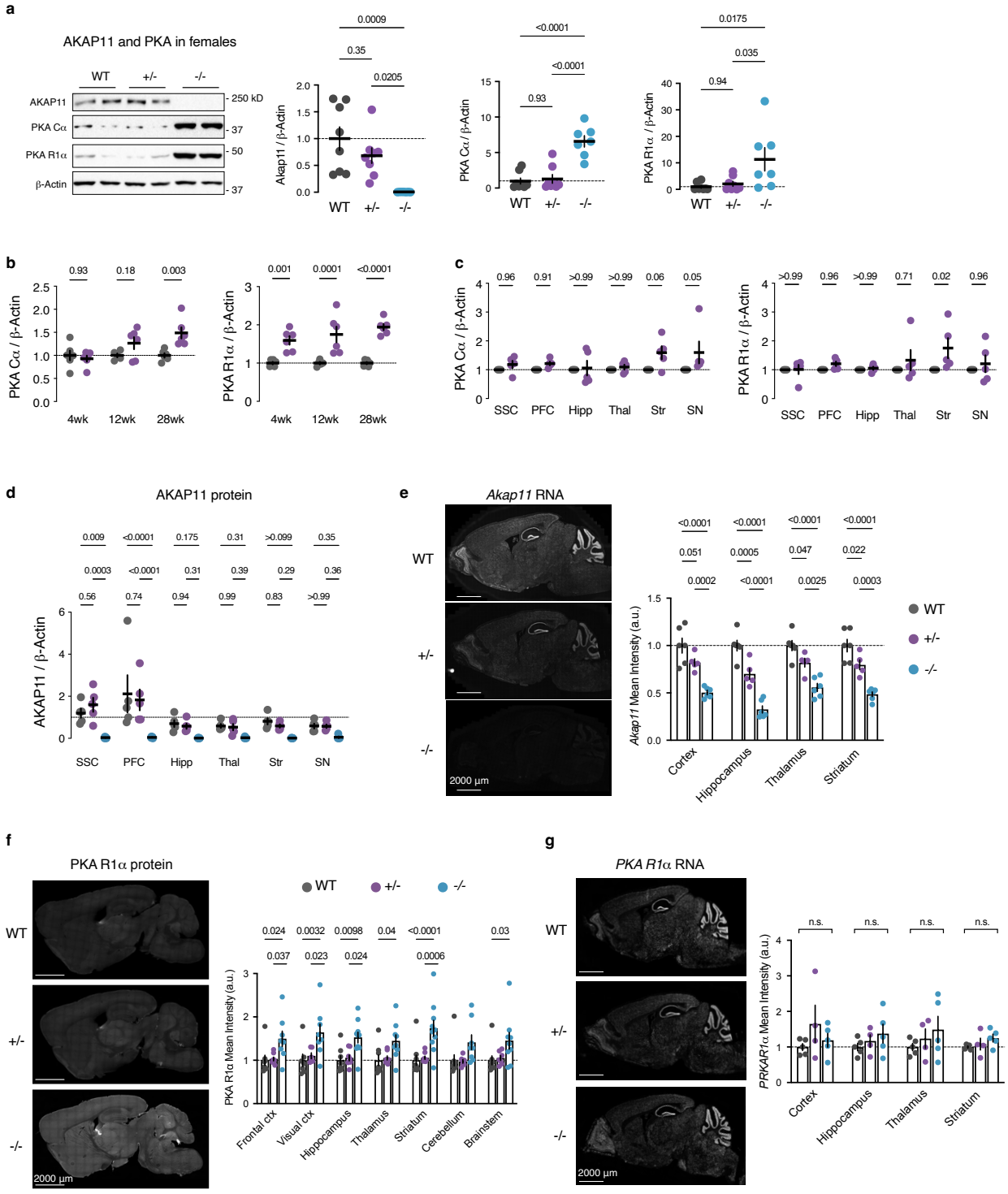

Supplementary Figure 3. PKA protein levels in *Akap11*$^{+/-}$ and *in situ*, related to Fig. 3.
a, Quantifications of AKAP11 and PKA subunit protein levels in female 12wk WT and *Akap11*$^{+/-}$ total lysate. One-way ANOVA with Tukey's post hoc test.
b,c, Quantifications of PKA subunit proteins levels in WT and *Akap11*$^{+/-}$ total lysate. These data are also shown in Fig. 3b,c, but are rescaled here without *Akap11*$^{-/-}$ for clarity. Two-way ANOVA with Sidak's post hoc test.

d, Quantification of immunoblots from microdissected tissue total lysate from 4wk mice using antibodies against AKAP11. Representative immunoblots for these measurements are shown in Fig. 3c. *P*-values are calculated without *Akap11*$^{-/-}$ in multiple comparisons. Unlike other figures, these data are not normalized to WT within a brain region, in order to display differences in AKAP11 protein across brain regions.
e, *In situ* hybridization measurements of *Akap11* RNA. Right, quantification of mean intensity measurements within anatomical subregions. Measurements are normalized to WT controls within a region.
f, Immunofluorescence measurements of PKA R1α protein *in situ*. Right, quantification of mean PKA R1α immunofluorescence intensity measurements within anatomical subregions. Multiple comparisons adjusted *P* values < 0.05 are displayed above.
g, *In situ* hybridization measurements of *PKA R1α* RNA. Right, quantification of mean intensity measurements within anatomical subregions. Measurements are normalized to WT controls within a region.
d-g, Two-way ANOVA with Tukey's post hoc test. See Supplementary Data 1 for statistics.
a-g, Data are represented as mean +/- SEM.

Supplementary Figure 4

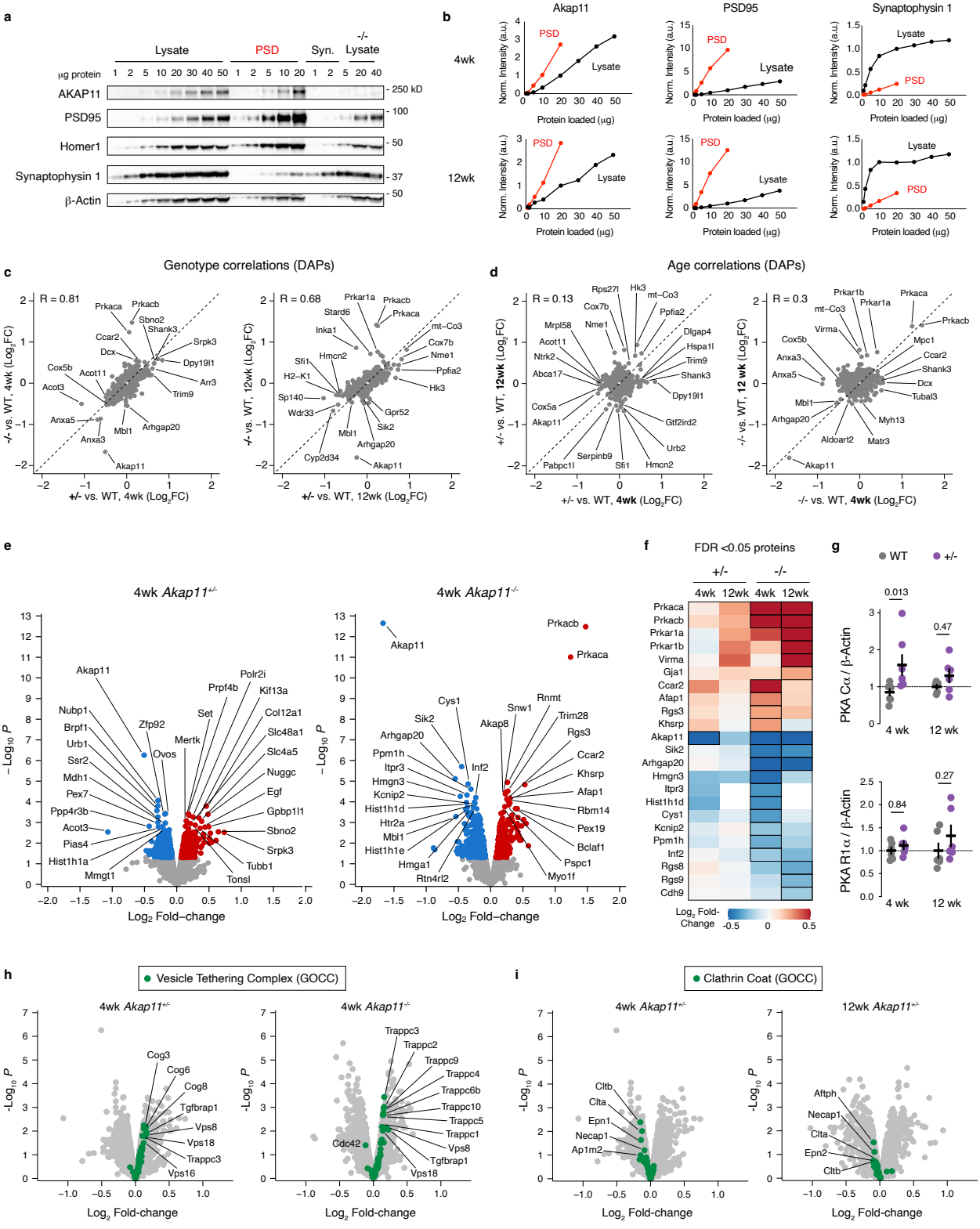

Supplementary Figure 4. Comparisons of juvenile and adult synapse proteomes, related to Fig. 4.
a, Immunoblots of AKAP11 and synapse proteins across different amounts of lysate, synaptosome, and PSD-enriched fractions of 12wk cortex.
b, Quantifications of immunoblots in (a). Values are normalized to 20µg lysate.
c, Log_2FC scatter plots comparing DAPs in *Akap11*$^{+/-}$ vs. *Akap11*$^{-/-}$ synapse proteomes.
d, Log_2FC scatter plots comparing DAPs in 4wk vs. 12wk synapse proteomes.
e, Volcano plots of 4wk synapse proteomics data. Upregulated and downregulated DAPs are colored red and blue, respectively.
f, Heatmap of adjusted *P*-value (FDR) < 0.05 proteins across 4wk and 12wk synapse proteomes. Black border indicates FDR significance, including corrections for comparisons between *Akap11*$^{+/-}$ and *Akap11*$^{-/-}$.
g, Quantifications of PKA subunit protein levels in WT and *Akap11*$^{+/-}$ synapse fractions. These data are also shown in Fig. 4c, but are rescaled here without *Akap11*$^{-/-}$ for clarity. Data are represented as mean +/- SEM. Two-way ANOVA with Sidak's post hoc test. See Supplementary Data 1 for statistics.
h, Volcano plots of 4wk synapse proteomics data in *Akap11*$^{+/-}$. Proteins within the Vesicle Tethering Complex gene set are highlighted in green.
i, Volcano plots of synapse proteomics data in *Akap11*$^{+/-}$. Proteins within the "Clathrin Coat" gene set are highlighted in green for 4wk and 12wk animals.

Supplementary Figure 5

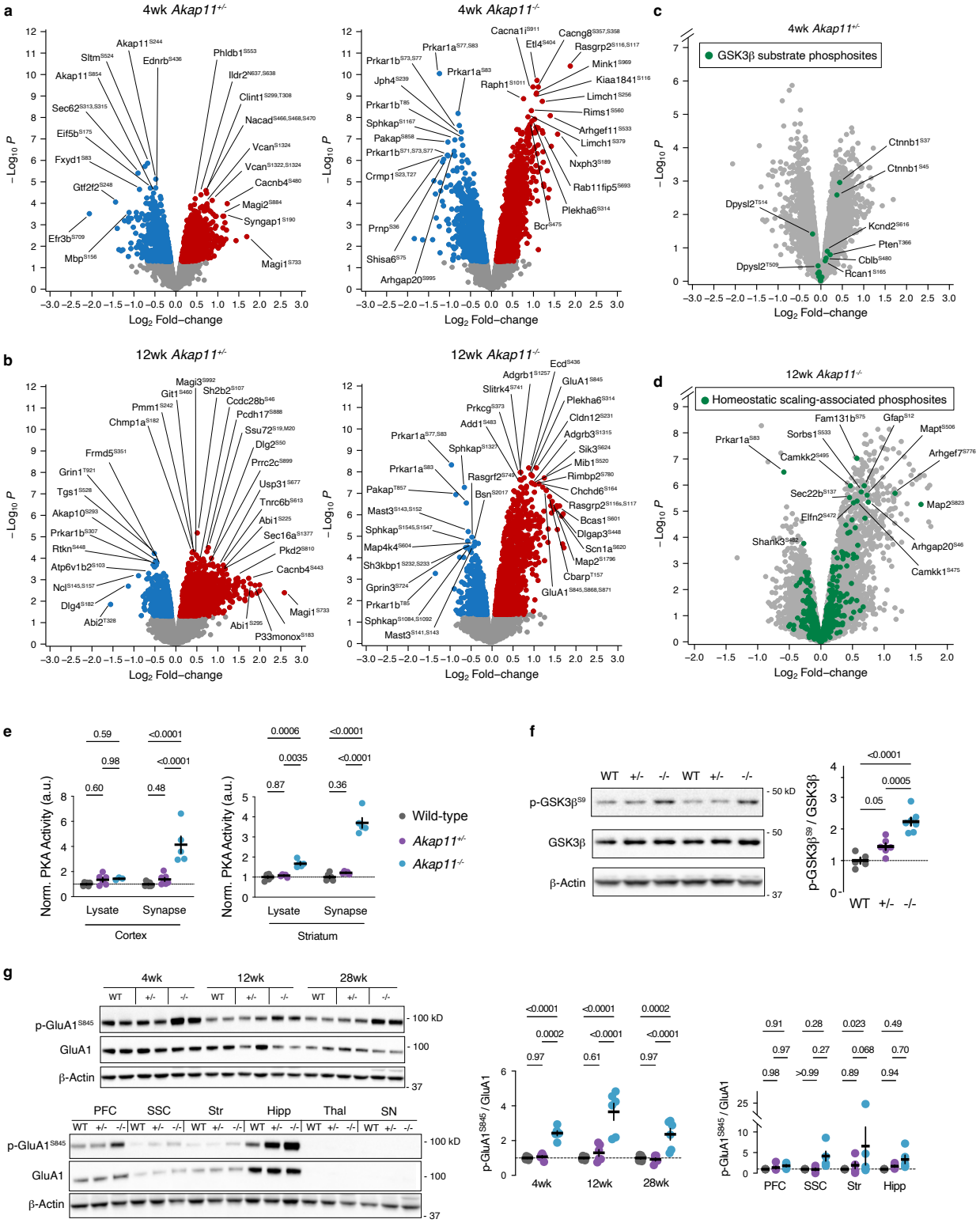

Supplementary Figure 5: Phosphoproteomic correlates of synaptic plasticity, related to Fig. 5.
a, Volcano plots of synapse phosphoproteomics in 4wk *Akap11* mutants relative to WT. Upregulated and downregulated DAPPs are colored red and blue respectively. AKAP11 phosphopeptides are omitted from *Akap11*$^{-/-}$ plots, for clarity.
b, Volcano plots of synapse phosphoproteomics in 12wk *Akap11* mutants relative to WT. Upregulated and downregulated DAPPs are colored red and blue respectively. AKAP11 phosphopeptides are omitted from *Akap11*$^{-/-}$ plots, for clarity.
c, Volcano plots of 4wk synapse phosphoproteomics for *Akap11*$^{+/-}$. Known GSK3β substrates from PhosphoSitePlus are labeled in green.
d, Volcano plots of 12wk synapse phosphoproteomics for *Akap11*$^{+/-}$. Phosphosites that are altered during scaling (24 hours of bicuculline or tetrodotoxin treatment, FDR <0.05 in Desch et al., 2021)[72] are labeled in green.
e, ELISA-based PKA activity measurements comparing total lysate and synapse fractions of cortex (left) and striatum-enriched tissue (right). These measurements appear in Fig. 5e, but have been normalized here to wild-type for more clear representation of fold-change. Two-way ANOVA with Tukey's post hoc test.
f, Immunoblotting and quantification of p-GSK3β^{S9} and GSK3β in 4wk cortical total lysate. One-way ANOVA with Tukey's post hoc test. See Supplementary Data 1 for statistics.
g, Immunoblotting and quantification of p-GluA1^{S845} and GluA1 in 4wk, 12wk or 28wk cortical or in microdissected brain region total lysate. Two-way ANOVA with Tukey's post hoc test. See Supplementary Data 1 for statistics.
.

Supplementary Figure 6

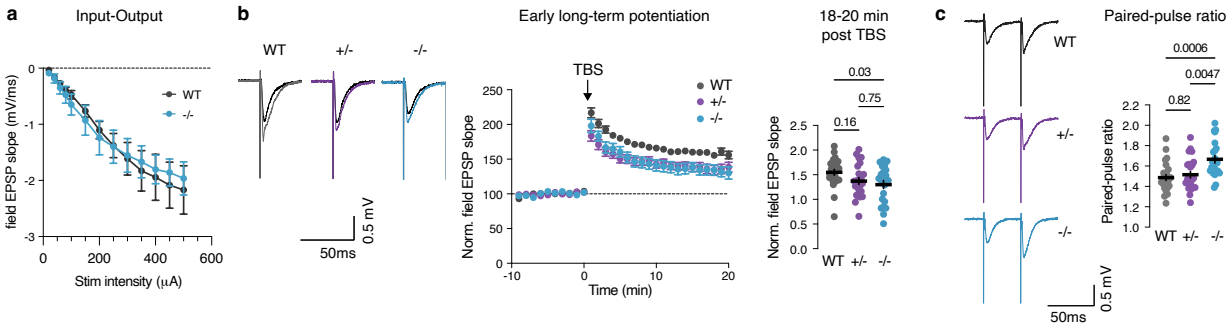

Supplementary Figure 6: Electrophysiological characterization of synaptic strength and plasticity, related to Fig. 5.
a, Input-output (I-V) curves of field excitatory postsynaptic potential (EPSP) responses evoked with varying stimulation intensities (20-500µA).
b, Left, representative traces of field EPSPs before and after LTP induced by theta burst stimulation (TBS). Traces were generated by averaging the data points during the first (baseline; light lines) and last (post LTP; dark lines) two mins of the experiment. Middle, quantification of field EPSP slopes over the 30-min long early LTP experiment. Each dot represents the average field EPSP slope over 1 min. Right, quantification of field EPSP slope in minutes 18-20 following TBS.
c, Left, representative traces of paired pulse responses at 40ms stimulation intervals. Right, quantification of paired pulse ratios from *Akap11* mutants and WT brain slices.
a-c, Data are represented as mean +/- SEM. One-way ANOVA with Tukey's post hoc test. See Supplementary Data 1 for statistics.

Supplementary Figure 7

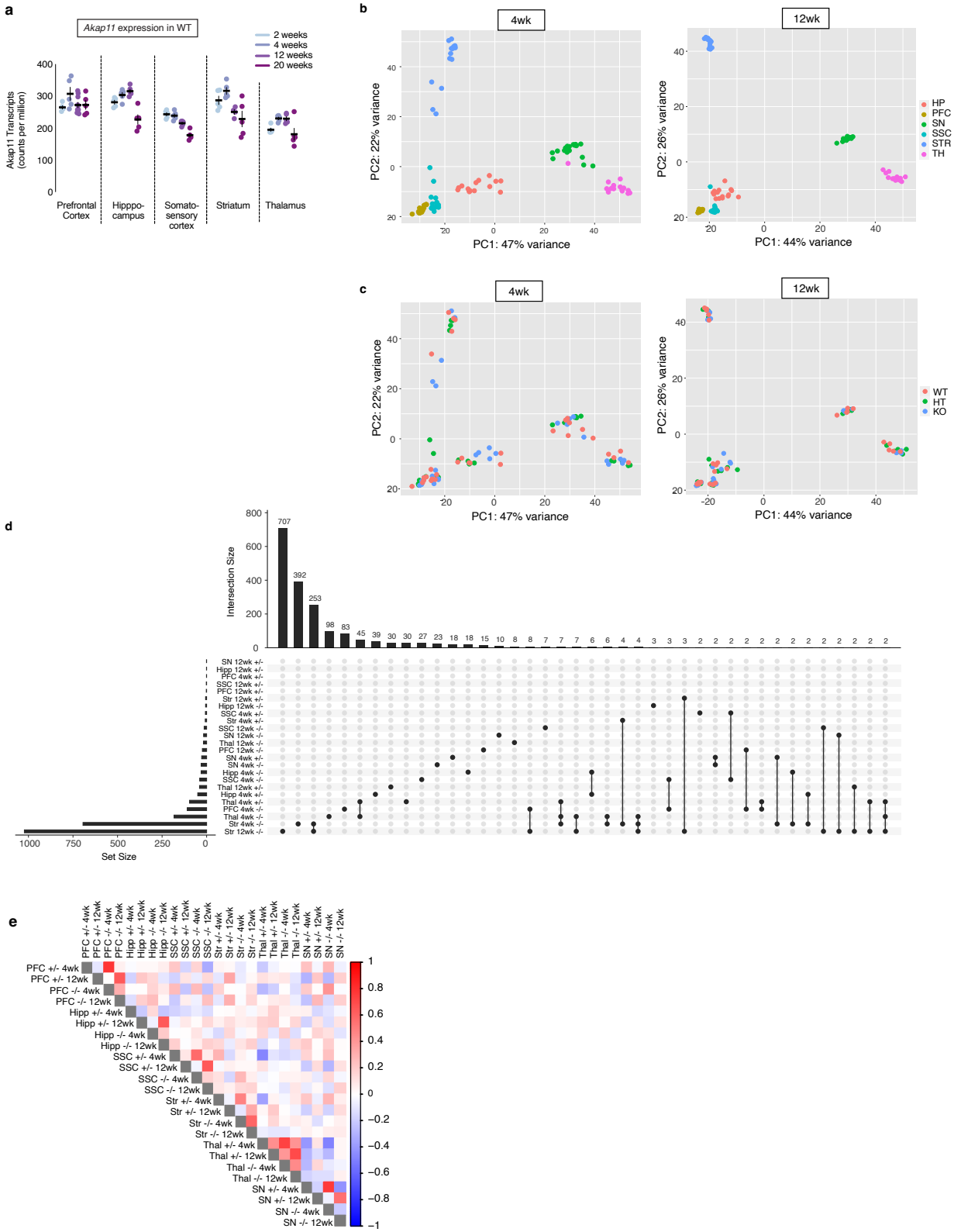

Supplementary Figure 7: Comparisons between brain regions, ages, and genotypes in bulk RNA sequencing, related to Fig. 6.
a, *Akap11* mRNA expression across brain regions and ages in wild-type mice, analyzed from data published in Farsi et al., 2023[12]. Data are represented as mean +/- SEM.
b, PCA plots of bulk RNA sequencing experiments, colored by brain region.
c, PCA plots of bulk RNA sequencing experiments, colored by genotype.
d, Upset plot showing overlapping and unique DEGs (FDR < 0.05) across brain regions, ages and genotypes in bulk RNA sequencing experiments.
e, Log_2FC correlations between nominally significant genes ($P < 0.05$) across brain regions, ages, and genotypes. Color indicates Spearman correlation values.

Supplementary Figure 8

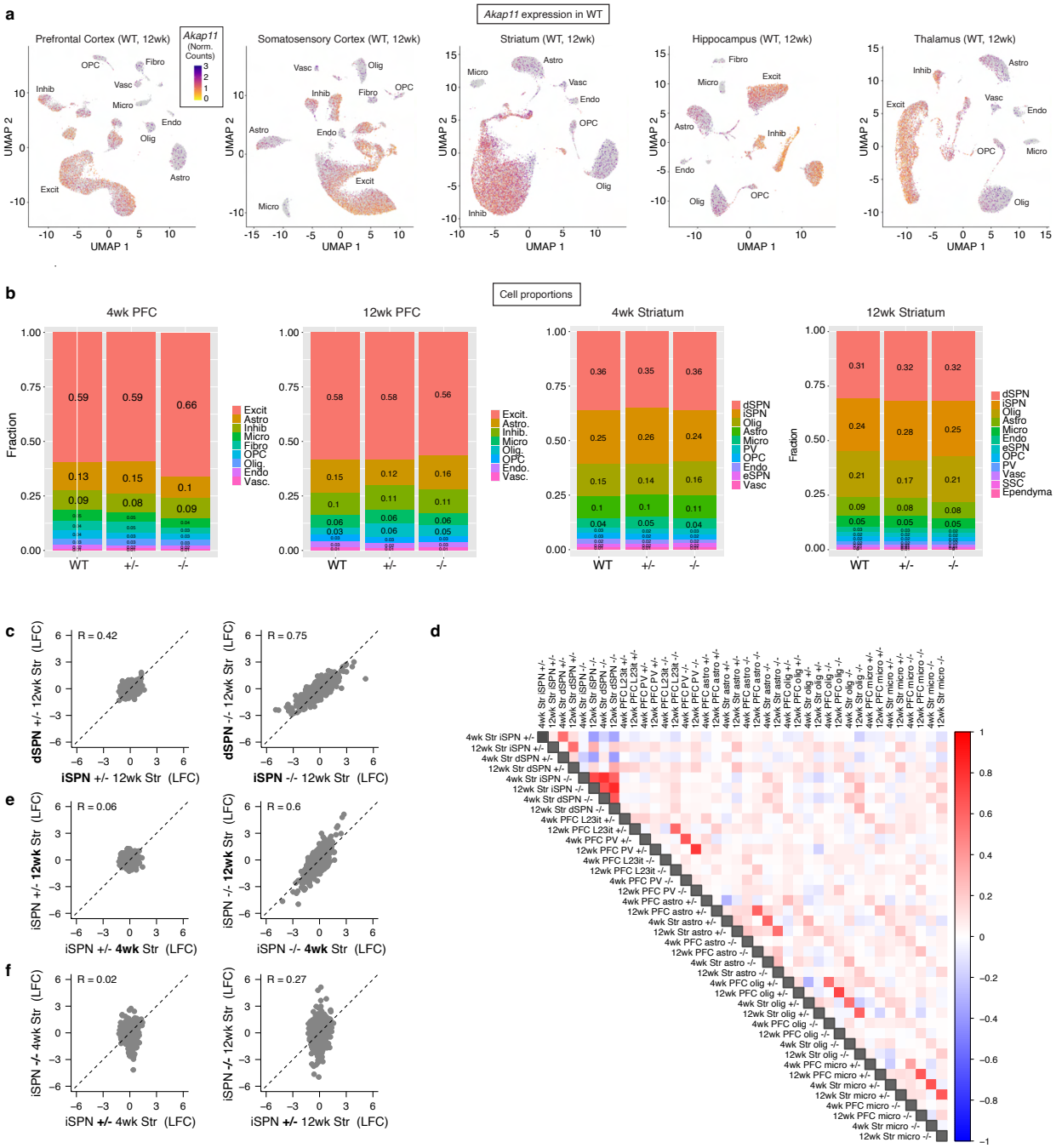

Supplementary Figure 8: Comparisons between brain regions, age and cell types in snRNA-seq, related to Fig. 6.
a, *Akap11* expression across major cell types on uniform manifold approximation and projection (UMAP) representations of cell types in different brain regions and ages of wild-type mice. These data appears in Farsi et al., 2023[12].
b, Fraction of each cell type identified across genotypes.
c, Log_2FC scatterplots comparing all genes for iSPN vs dSPN subtypes.
d, Log_2FC correlations between nominally significant genes ($P < 0.05$) across cell types. Color indicates Pearson correlation values.
e, Log_2FC scatterplots comparing all genes at 4wk vs. 12wk, in iSPNs.
f, Log_2FC scatterplots comparing all genes in *Akap11*$^{+/-}$ vs. *Akap11*$^{-/-}$, in iSPNs.

Supplementary Figure 9

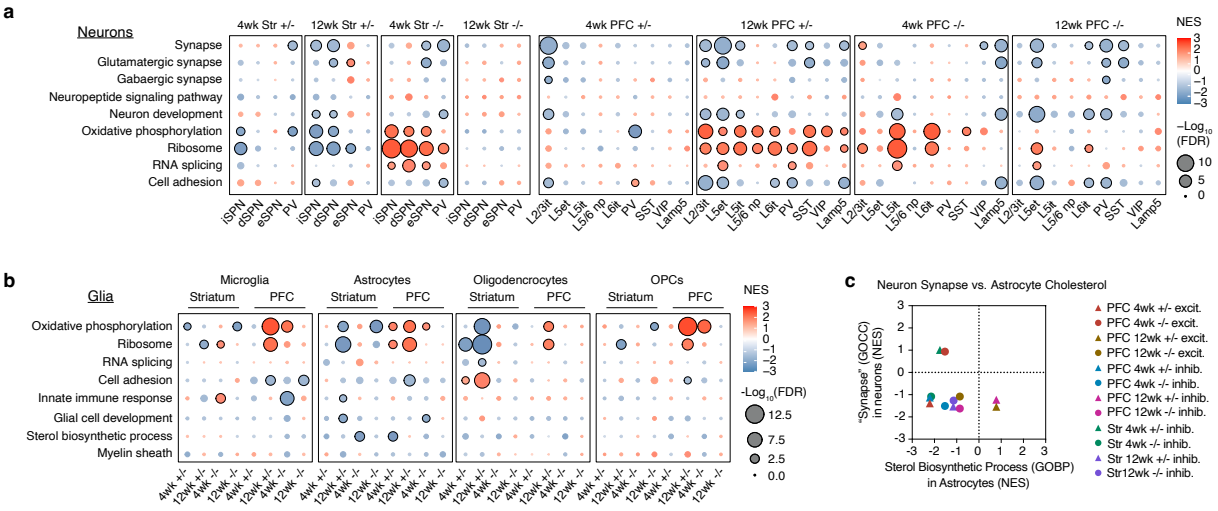

Supplementary Figure 9: Neuronal-synapse and astrocyte-cholesterol related transcriptomic changes detected by snRNA-seq, related to Fig. 6.

a, GSEA from neurons identified by snRNA-seq of striatum and PFC, showing MsigDB pathways of interest.

b, GSEA results from glia snRNA-Seq, showing, showing MsigDB pathways of interest, including pathways related to glia function.

c, Comparison of NES from synapse pathways in neurons vs. cholesterol biosynthesis pathways in astrocytes.

Supplementary Figure 10

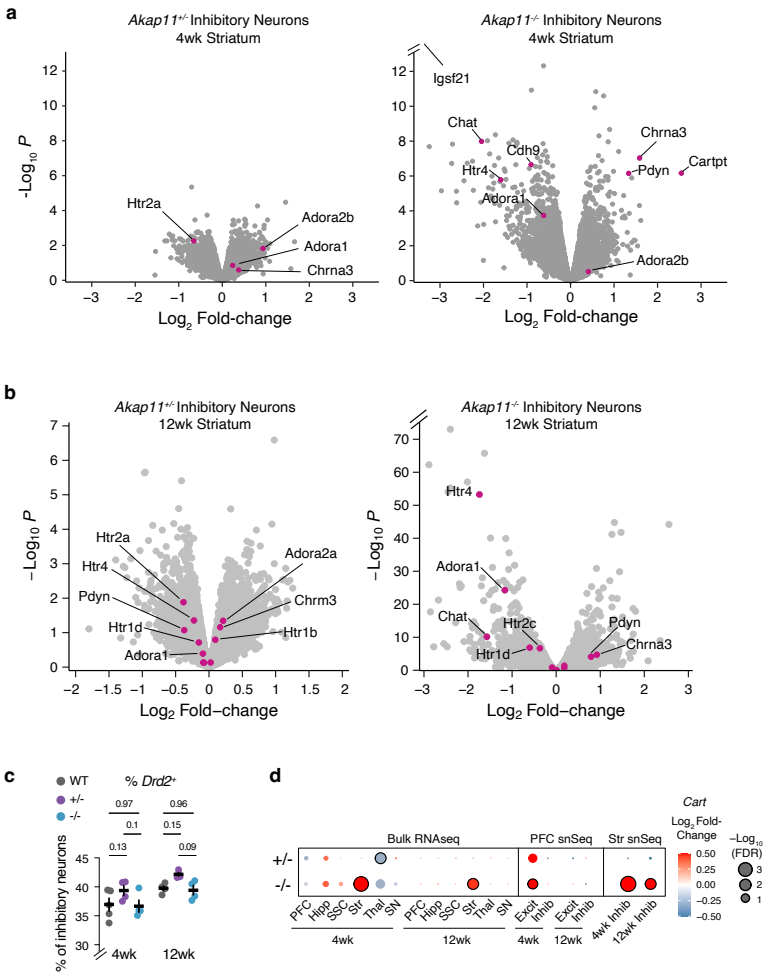

Supplementary Figure 10: Evidence for transcriptomic alteration of neuromodulation-related genes, related to Fig. 6.
a, Volcano plots of transcriptomic changes identified by snRNA-seq analysis in 4wk striatal inhibitory neurons. Genes of interest related to neuromodulation and circuit development are highlighted in magenta.
b, Volcano plots of transcriptomic changes identified by snRNA-seq analysis in 12wk striatal inhibitory neurons. Genes of interest related to neuromodulation and circuit development are highlighted in magenta.
c, Percentage of $Drd2^+$ inhibitory neurons in the striatum. Data are represented as mean +/- SEM. Two-way ANOVA with Tukey's post hoc test.
d, Log_2FC and FDR-adjusted *P*-values for *Cart* across bulk and snRNA-seq.

Supplementary Figure 11

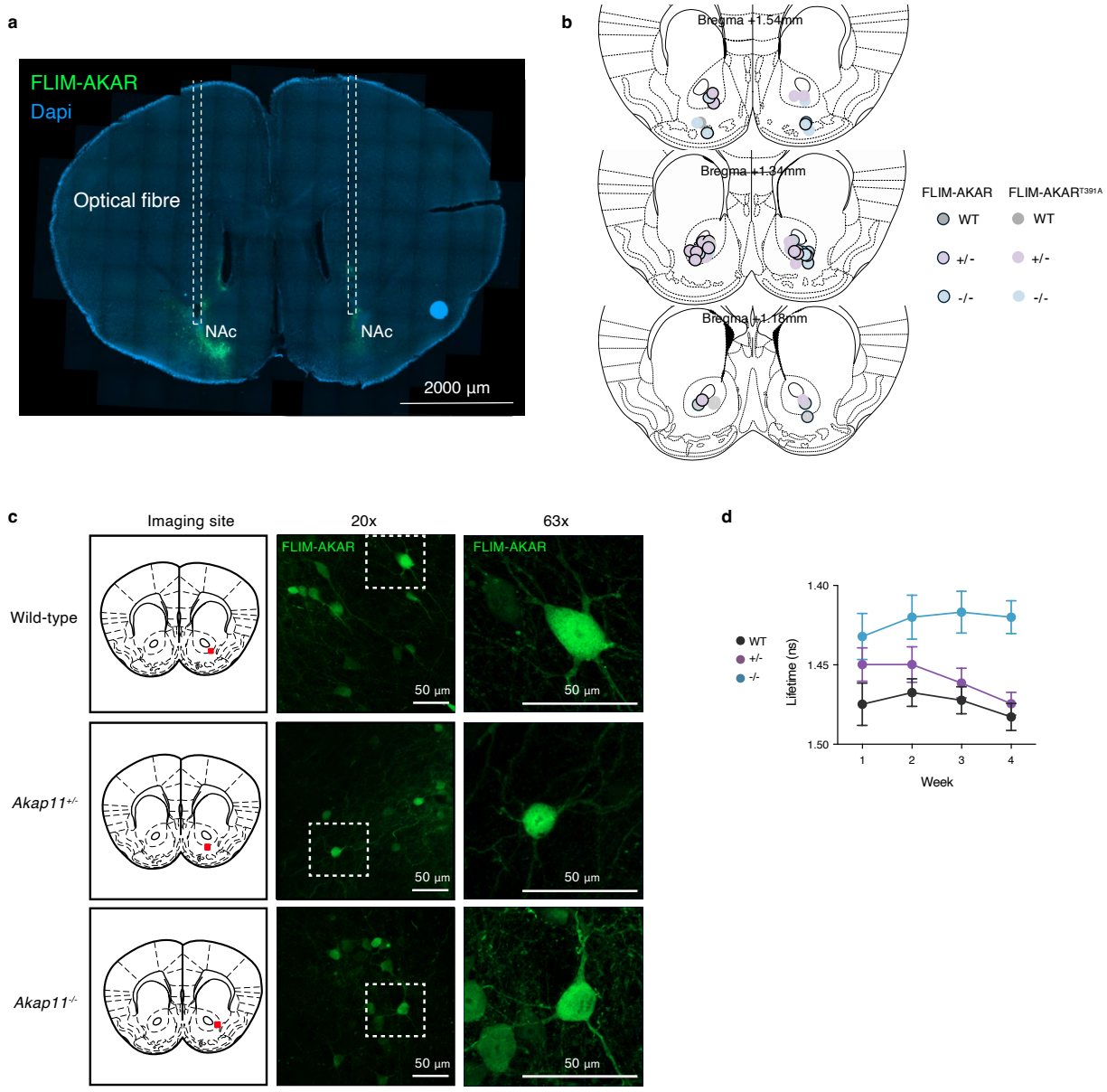

Supplementary Figure 11: FLIM-AKAR injections sites and longitudinal measurement of PKA activity, related to Fig. 7.
a, Immunohistochemical validation of AAV injection site targeting of NAc.
b, Injection site targets of each animal in this study. Animals of different genotypes are differentiated by color, and FLIM-AKAR variants that were injected into contralateral hemispheres are differentiated by black border.
c, Native fluorescence of FLIM-AKAR, imaged under a confocal microscope. Left, schematic of approximate imaging site.
d, Fluorescence lifetime of FLIM-AKAR across 4 fiber photometry recording sessions across weeks.

Supplementary Figure 12

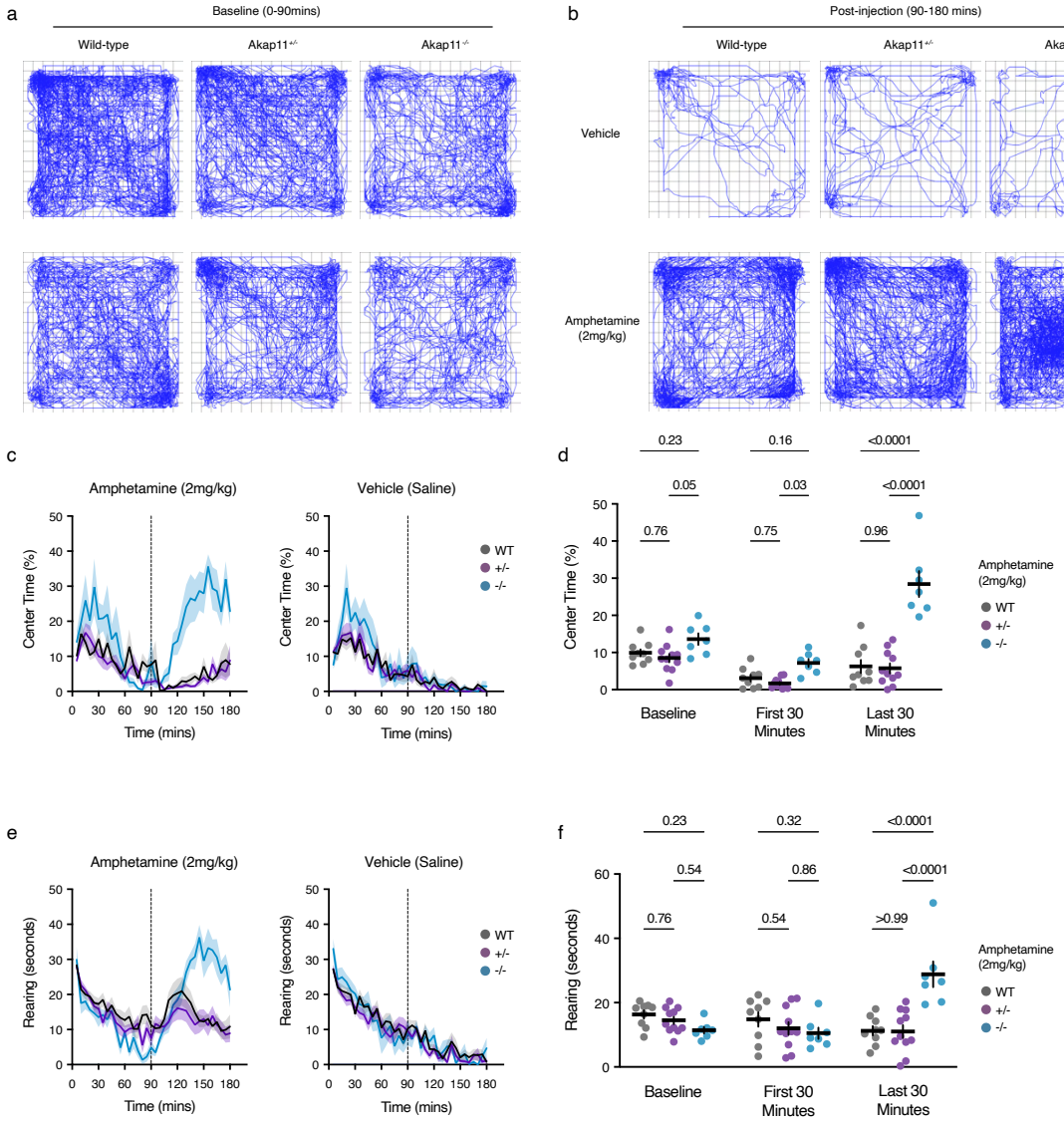

Supplementary Figure 12: Amphetamine induces excessive open-field center time and rearing behaviors in *Akap11*$^{-/-}$ mice, related to Fig. 7

a,b, Representative activity traces of mice in the open field arena, before **(a)** and after **(b)** amphetamine (2 mg/kg) or saline administration. The same animals are shown in **(a)** and **(b)**, before and after vehicle (top rows) or amphetamine (bottom rows) administration.

c, Centre time (%) after administration of amphetamine or saline to WT or *Akap11* mutants.

d, Quantification of center time (%) during baseline (0-90mins), first 30 minutes post injection (90-120mins), and during the last 30 minutes (150-180mins) of the trial. Repeated measures two-way ANOVA with Tukey's post hoc test. See Supplementary Data 1 for detailed statistics.

e, Rearing time (s) after amphetamine (2 mg/kg) or saline administration to WT or *Akap11* mutants.

f, Quantification of rearing time (s) during baseline (0-90mins), first 30 minutes post injection (90-120mins), and during the last 30 minutes (150-180mins) of the trial. Repeated measures two-way ANOVA with Tukey's post hoc test. See Supplementary Data 1 for detailed statistics.